JOURNAL OF CATALYSIS **180,** 258–269 (1998)
ARTICLE NO. CA982275

Zeolite Catalysts for the Selective Synthesis of Mono- and Diethylamines

Victor A. Veefkind and Johannes A. Lercher[1]

Faculty of Chemical Technology, University of Twente, P.O. Box 217, 7500 AE, Enschede, The Netherlands

Received June 19, 1998; revised September 2, 1998; accepted September 2, 1998

The kinetics and mechanism of ethylamine synthesis from ammonia and ethanol over several large pore acid catalysts are described. Mordenite produced higher monoethylamine yields than the zeolites beta, Y, mazzite, and amorphous silica–alumina. The reaction proceeds via the initial formation of ethylammonium ions, and alkylamines desorb with the assistance of ammonia and equilibrate with other ethylammonium ions before leaving the catalyst pores. The high yields of ethylamines with mordenite are related to the high acid strength of the catalyst stabilizing (alkyl)ammonium ions and so blocking the dehydration of ethanol. By choosing high ammonia partial pressures, reaction temperatures below 573 K (minimizing ethene elimination from ethylammonium ions), and subtle modifications of the parent mordenite material (EDTA leaching, silylation of the external surface) ethene selectivity was further decreased. These measures allowed us to prepare a catalyst on the basis of mordenite with a Si/Al ratio of 5 that showed 99% selectivity to ethyl amines at 60% conversion and that was stable for long times on stream.

Key Words: **large pore zeolites; ethylamine synthesis; shape selective amination.**

INTRODUCTION

Alkylamines are widely used as intermediates in the synthesis of fine chemicals (1, 2). Conventionally alkylamines are produced via reductive amination of aldehydes or alkylation of ammonia over acidic silica/alumina (1, 2). Zeolites have attracted increasing attention as catalysts for the latter reaction route (3), as they display strong acidity and pronounced shape selectivity favoring primary and secondary amines.

Consequently, zeolite-catalyzed methylamine synthesis has been extensively studied (4–10), including a recent exhaustive review on this subject (3). One of the most successful zeolites used for this reaction is mordenite, and a significant number of papers and patents on the catalysis over mordenite have been published (see Ref. (3) and references therein). Treatment of mordenite with silylating agents has been shown to enhance the selectivity to methylamines in general and to lower substituted amines (mono- and dimethylamine) in particular. Such postsynthetic treatments are claimed to deactivate the outer surface of the mordenite crystallites and to reduce the size of the pore mouth (6, 11, 12). Along these lines, the selectivity enhancement to lower substituted amines can be explained by the inability of the trimethylamine (TMA) to leave the pores of the modified catalyst and by enhancement of the probability that TMA in the mordenite pores disproportionates with ammonia or monomethylamine (MMA) to dimethylamine (DMA), the desired product (6, 12). A surprising side effect is the significant decrease in formation of dimethylether (DME), the main side product, after silylation (12, 13).

The direct amination of ethanol to ethylamines has been much less discussed in the literature, but reports indicate that zeolites Y (FAU), ZSM-5 (MFI), erionite (ERI), mordenite (MOR), and beta (BEA) (14–16) are active catalysts. The biggest challenge in ethylamine synthesis is to achieve high selectivities with respect to ethanol use. The formation of diethyl ether (DEE) and ethene should be avoided, as ammonia and ethene are difficult to separate (complicating the recycle), and ethene may deactivate the zeolite via oligomerization.

Formation of ethene from ethanol is thermodynamically favored under most reaction conditions applied, as illustrated in Fig. 1. In Fig. 1a the equilibrium product distribution between monoethylamine (MEA), diethylamine (DEA), triethylamine (TEA), ammonia, water, and ethanol at 1 bar is shown starting from 1 mol ethanol and 4 mol ammonia. Formation of amines is favorable, although it should be noted that thermodynamics limit the conversion of ethanol to 97% at 573 K. Figure 1b also shows the equilibrium product distribution between the various molecules, but unlike in Fig. 1a, the formation of ethene is now permitted. One notes that ethanol can be almost completely converted to ethene at temperatures above 550 K. Thus, ethene formation has to be kinetically blocked in order to achieve a useful ethanol utilization.

The present contribution aims at providing evidence for the main elementary steps of the alkylation of ammonia with ethanol using combined *in situ* IR spectroscopy and kinetic measurements. This knowledge is used to tailor a

[1] To whom correspondence should be addressed. Fax: 31-53-4894683. E-mail: j.a.lercher@ct.utwente.nl.

0021-9517/98 $25.00

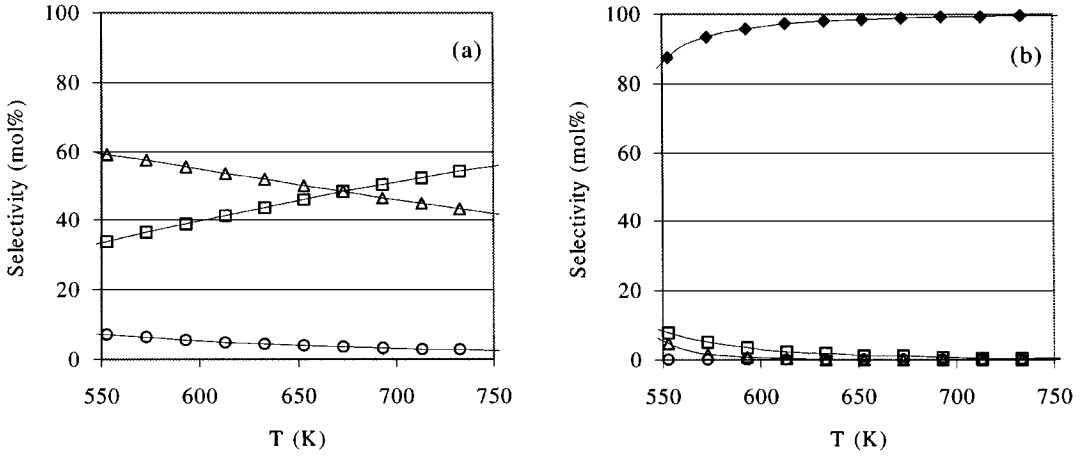

FIG. 1. Dependence of the equilibrium product distribution on reaction temperature at $NH_3/EtOH = 4$ and $p = 1$ bar (a) without ethene present and (b) with ethene formation. (□) MEA, (△) DEA, (○) TEA, (◆) ethene.

mordenite-based catalyst for achieving maximum ethylamine yield.

EXPERIMENTAL

Brønsted acidic mordenites with a Si/Al ratio of 10 (HMOR20), 7.5 (HMOR15), and 5 (HMOR10) were obtained from the Japanese Catalysis Society (17). HMOR10-E was obtained by treating a Na-MOR (NaMOR10) with EDTA solution, followed by calcination and ion exchange with NH_4NO_3. The reason for this treatment was the anomalously low pore volume of 0.05 cm^3/g for HMOR10, which was restored to 0.10 cm^3/g for HMOR10-E (18). HMOR20-M, HMOR15-M, and HMOR10-EM were prepared by adding tetraethoxysilane to a suspension of the activated MOR in *n*-hexane (25 ml/g zeolite), followed by intense stirring at room temperature, removal of the solvent, and subsequent calcination in air. The amount of tetraethoxysilane was calculated to result in a weight gain of 4% by externally deposited SiO_2 (12). BEA with a Si/Al ratio of 11 was obtained from PQ Corporation (19). FAU with Si/Al = 2.7 was supplied by Ventron. The silica–alumina was LA-C25W from Akzo–Nobel (Si/Al = 3.5).

The physicochemical data for the catalysts used are compiled in Table 1. The BET surface area and the micropore volume of the catalysts were measured on a Micromeritics Accelerated Surface Area Porosimeter (ASAP 2400). The concentration of extraframework aluminum (EFAL) was determined by ^{27}Al MAS NMR (19). The concentration of strong Brønsted acid sites was calculated from the gravimetrically determined amount of irreversibly adsorbed ammonia after sorption and subsequent evacuation at 373 K for 10 h at a pressure of 10^{-6} mbar (18). These gravimetric measurements were performed on a TGA/DSC system consisting of a SETARAM TG-DSC 111 instrument connected to a high vacuum system (20). The values for EFAL

TABLE 1

Physicochemical Properties of the Investigated Brønsted Acidic Mordenites

Catalyst	Specific area (m^2/g)	Micropor. vol. (cm^3/g)	Si/Al	EFAL (%)	Brønsted acid sites (mol/g)	Calculated Al content (mol/g)
HMOR20-M	353	0.15	10	10	1.1×10^{-3}	1.1×10^{-3}
HMOR20	390	0.21	10	n.d.	1.3×10^{-3}	1.3×10^{-3}
HMOR15-M	390	0.17	7.5	~10–15	1.5×10^{-3}	1.7×10^{-3}
HMOR15	350	0.15	7.5	11	1.7×10^{-3}	1.8×10^{-3}
HMOR10-EM	360	0.12	6	~10–15	1.9×10^{-3}	2.0×10^{-3}
HMOR10-E	280	0.10	6	n.d.	2.0×10^{-3}	2.1×10^{-3}
HMOR10	130	0.05	5	8	2.1×10^{-3}	2.3×10^{-3}
HMAZ	330	0.12	10	n.d.	$\sim 1.2 \times 10^{-3}$	1.3×10^{-3}
HFAU	758	0.34	2.7	n.d.	3.0×10^{-3}	3.0×10^{-3}
HBEA	514	0.11	11	38	0.7×10^{-3}	1.2×10^{-3}

Note. n.d., not detected (<5%).

found with ^{27}Al MAS NMR are consistent with the difference between calculated Al concentration and the measured Brønsted acid site concentration.

For adsorption/coadsorption measurements, a Bruker IFS88 FTIR spectrometer was equipped with a vacuum cell. This high vacuum cell consisted of a stainless steel chamber equipped with CaF_2 windows and a resistance-heated furnace in which a gold sample holder was placed. To analyze desorbing gasses the system was equipped with a Balzers QMG 420 Mass spectrometer. The base pressure of the system was 10^{-6} mbar. Reactants were introduced to the system with a pressure of 10^{-3} mbar, using a dosing valve. Spectra were taken at a resolution of 4 cm^{-1}.

Under reaction conditions the IR spectra were recorded *in situ* using a Nicolet 20SXB FTIR spectrometer in the transmission absorption mode with a resolution of 4 cm^{-1}. An *in situ* IR cell was used in combination with gas chromatography to allow simultaneous analysis of sorbed species and products (for details see Ref. (21)). Typically 3 mg of the catalyst was pressed into a self-supported wafer and activated in He flow for 1 hr at 823 K and then cooled to reaction temperature.

For measurements at higher conversion a quartz plug flow reactor was used in combination with a GC equipped with FID and TCD. A Restek RTX amine column was used for separation. Typical reaction conditions were 573 K and 40 mbar ethanol and 160 mbar ammonia or 100 mbar ethanol and 800 mbar of ammonia, balanced with He to atmospheric pressure. The specific conditions in each experiment are reported under Results.

The chemicals used for these experiments were ethanol (p.a. grade) obtained from Merck, ammonia gas (Praxair, 99.999% pure), and a mixed gas containing 19.5% NH_3 in He (Praxair, 99.999% pure).

RESULTS

Coadsorption of Ammonia and Ethanol

The formation of surface species under nonreactive conditions was studied by coadsorption of ammonia and ethanol at ambient temperature. These coadsorption experiments were carried out at partial pressures of 1×10^{-3} mbar for both components using a differentially pumped inlet system. First, one compound was adsorbed until full coverage was reached and then the second was introduced, while maintaining the partial pressure of the first compound. During coadsorption experiments the same equilibrium state was reached, regardless of the sequence of adsorption of the two adsorbates. The spectra of ammonia sorbed on HMOR20, ethanol sorbed on HMOR20, and their coadsorption are shown in Fig. 2. Also shown is the difference between the spectrum of the coadsorbed species and the spectrum of ammonia sorbed on HMOR20. Upon sorption of ethanol, bands appeared at 2984 and 2917 cm^{-1} (attributed to asymmetric and symmetric CH_3 stretching vibrations) and bands at 2939 and 2880 cm^{-1} (attributed to asymmetric and symmetric CH_2 stretching vibrations). Additional broad bands at 3500, 3290, 2920, and 2400 cm^{-1} and an intense band between 1900 and 1400 cm^{-1} were observed. These bands are attributed to O–H stretching and

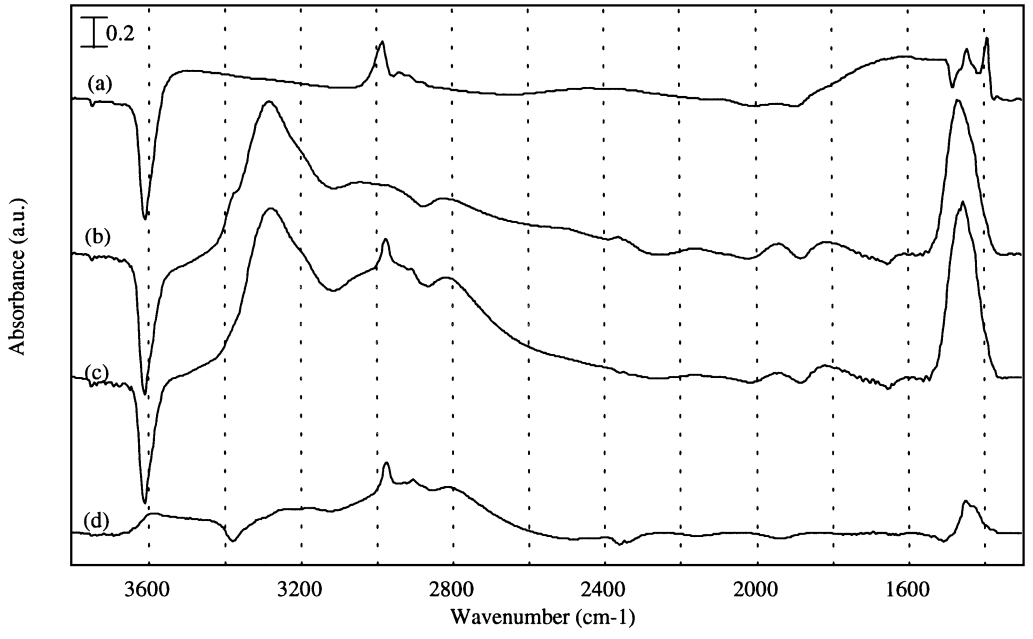

FIG. 2. IR spectra of (a) ethanol, (b) ammonia, and (c) ammonia and ethanol adsorbed on H-MOR20. (d) Difference between (c) and (b). p_{NH3}, $p_{EtOH} = 10^{-3}$ mbar, $T = 300$ K.

deformation vibrations from strongly bound methanol molecules (22–25). Sorption of ammonia gave rise to bands at 3378, 3300, 3200, 3050, 2964, and 2800 cm^{-1} together with an intense band at 1465 cm^{-1}, all characteristic for sorbed ammonium ions (26, 27). The multiple N–H stretching bands and the slightly asymmetric shape of the 1465 cm^{-1} band suggest different acid sites or more than one orientation of the ammonium ions with respect to the zeolite lattice. The shoulder at 3378 cm^{-1} is assigned to a free N–H stretching vibration from ammonium ions. This shoulder disappears upon coadsorption with ethanol, which can also clearly be seen in the difference spectrum (negative band at 3378 cm^{-1}). This indicates that ethanol and ammonium ions interact. The additional band at 3600 cm^{-1} is assigned to the O–H stretching vibration of coadsorbed ethanol. Its position in the spectrum is similar to that of alcohol O–H bands sorbed on alkali ion-exchanged zeolites (28). The ammonium N–H deformation band did not decrease upon ethanol coadsorption, indicating that ethanol adsorbs on top of or next to ammonium ions, but does not replace the ammonia from Brønsted acid sites.

Upon coadsorbing ammonia onto a zeolite pre-equilibrated with ethanol the bands attributed to ethanol interacting with the Brønsted acid sites of the zeolite disappeared. All bands attributed to protonated ammonia appeared with exception of the shoulder at 3378 cm^{-1} attributed to the free N–H band. The spectrum of this coadsorption complex obtained was identical to the spectrum obtained when starting with the ammonia pre-equilibrated zeolite shown in Fig. 2.

Subsequently, the sample was evacuated and the temperature was increased by 10 K min^{-1} while monitoring the adsorbates by IR spectroscopy and the desorbed products by mass spectrometry. The results are shown in Fig. 3. Below 500 K desorption of ethanol was observed, followed by a release of ammonia starting between 550 and 600 K which was accompanied by the reappearance of the bands of the zeolite OH groups. This confirms that the ethanol interacts with the ammonia but not directly with the Brønsted acid site.

Temperature-programmed desorption (TPD) of ethylamines from Brønsted acidic mordenites in all three cases showed a reactive desorption of the amine, i.e., the

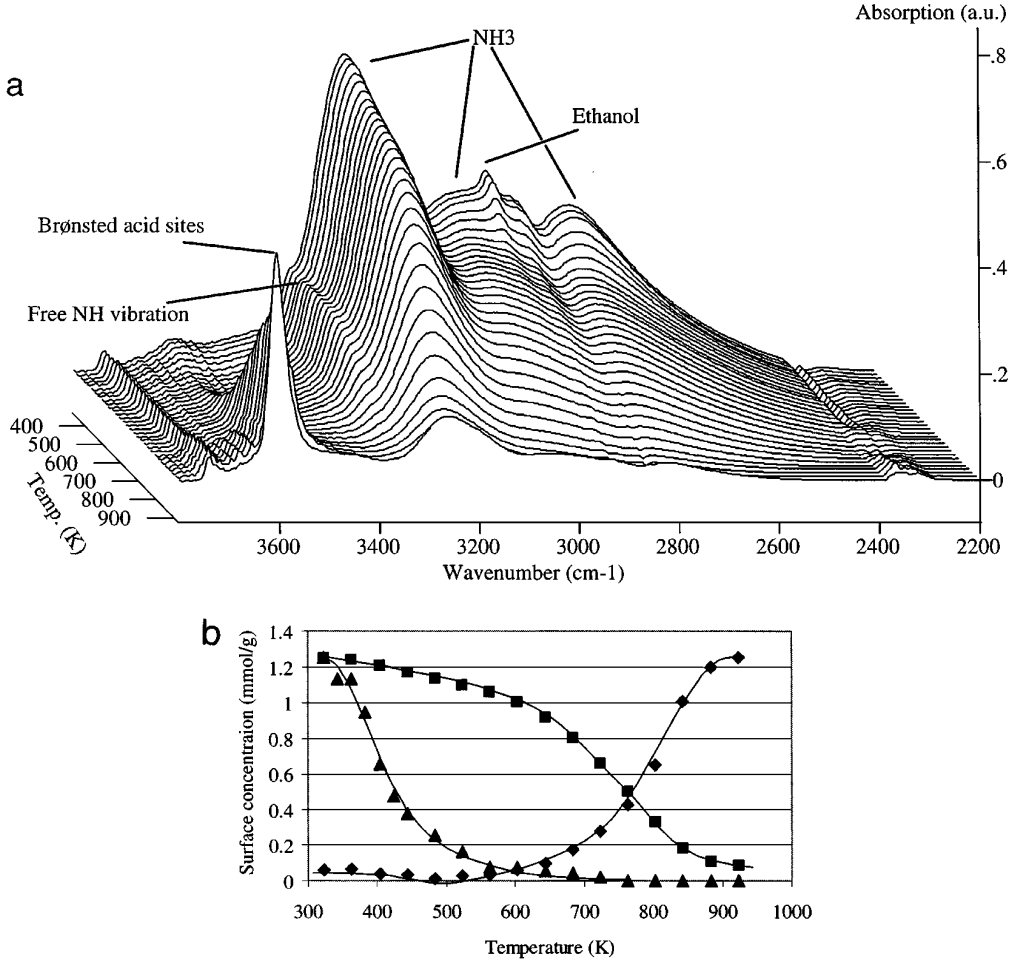

FIG. 3. (a) IR spectra during TPD of coadsorbed species. (b) Surface coverage of MOR20 with (▲) ethanol, (■) ammonia, and (◆) Brønsted acid sites during TPD of coadsorbed species.

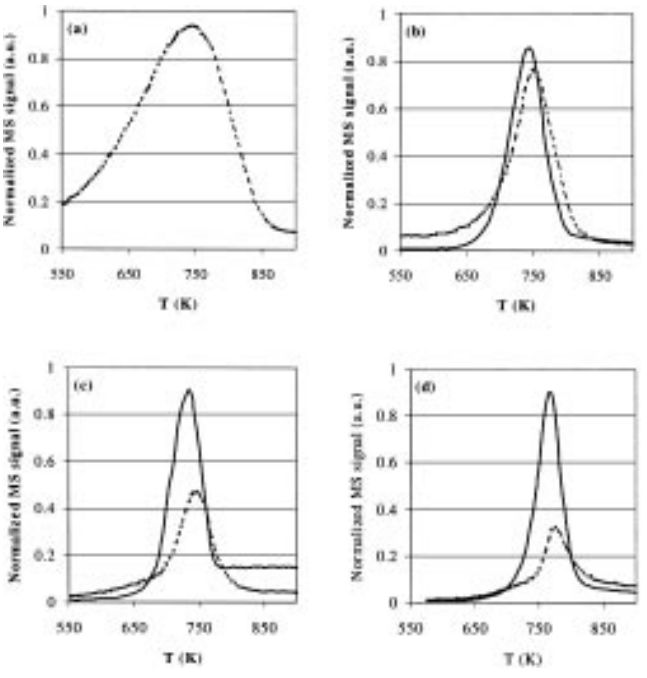

FIG. 4. Temperature-programmed desorption of (a) ammonia, (b) MEA, (c) DEA, and (d) TEA from H-MOR20. Dashed line, ammonia; solid line, ethene.

decomposition of the amine into ethylene and ammonia at temperatures above 573 K, as was also described for other alkylamines (see Ref. (32)). The corresponding TPD traces are shown in Fig. 4. The relative intensity of the ethene peak vs the ammonia peak correlated well to the substitution of the ethylamine. With increasing alkyl substitution the onset of the ammonia desorption shifted to higher temperatures (from 550 K for NH_3, 680 K for MEA, 700 K for DEA, to 740 K for TEA), indicating that the amines first undergo decomposition (Hofmann elimination of ethylene from the ethylamines) before ammonia desorbs. This is consistent with the higher base strength and hence the higher stability of the ammonium ions of the ethylamines compared to ammonia. It should be emphasized at this point that the amine decomposition limits the potential reaction temperature as it opens a pathway to ethene formation.

Reaction of Ammonium Ions with Ethanol

In order to investigate the reaction pathway, NH_4-MOR was contacted with a stream of ethanol (40 mbar ethanol, 6 ml/min, 3 mg zeolite) at 573 K, while analyzing the zeolite, adsorbates and reaction products with *in situ* IR spectroscopy. Upon contact with ethanol the ammonium ions rapidly disappeared and a mixture of ethylammonium ions appeared. Steady state was reached in less than 20 min. Figure 5 shows the spectrum of the ammonia saturated MOR and after contacting this sample with 40 mbar EtOH for 30 min. The bands attributed to the ethylammonium ions (3005–2875 cm^{-1}, C–H stretching vibrations; 2850–2400 cm^{-1}, combination bands typical for amines; 1610–1395 cm^{-1}, N–H and C–H deformation vibrations) quickly developed. By gas chromatography only ethene and diethyl ether (DEE) were detected as reaction product. At longer time on stream also some other hydrocarbons, but no amines were observed.

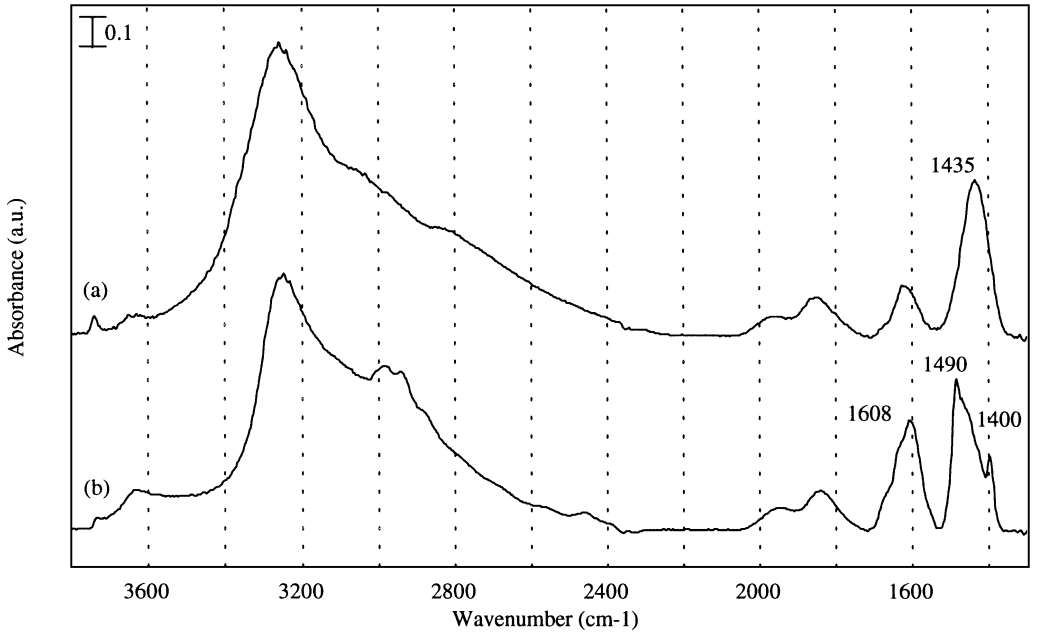

FIG. 5. In situ IR spectra of (a) ammonium mordenite and (b) catalyst after contacting for 30 min with 40 mbar ethanol/He ($T = 573$ K), showing adsorbed ethylammonium ions.

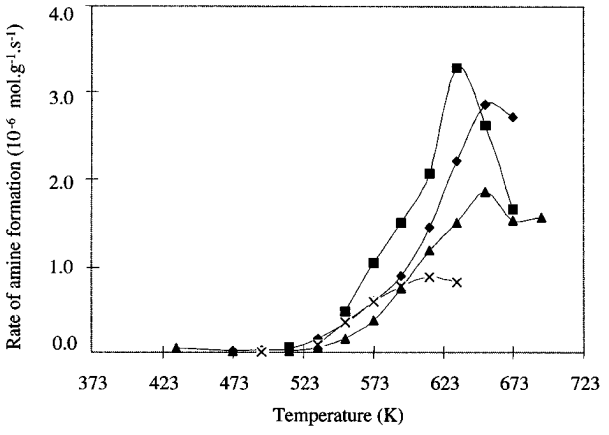

FIG. 6. Rate of MEA formation vs temperature for different catalysts. (■) HMOR15, (◆) BEA, (▲) MAZ, (×) FAU.

After 90 min purging with He at the same temperature, ammonia was passed over the loaded catalyst. This resulted in the appearance of amines in the gas phase as detected by gas chromatography, indicating that the presence of ammonia is indispensable for their catalytic formation. The rate of amine release form the zeolite pores was two to three times lower than the rate of formation of the methylammonium ions. This suggests that the rate of ammonia-aided amine release is rate determining. MEA was the favored product; TEA was hardly detected which could be seen as a consequence of the excess of ammonia under these particular reaction conditions.

Amination of Ethanol over Acid Zeolites

When introducing ammonia and ethanol simultaneously to a freshly activated H-MOR sample, initially high rates of ethene and DEE formation were observed. This was attributed to a chromatographic effect in which initially ammonia was retained at the entrance of the catalyst bed, giving the ethanol the chance to react with the free Brønsted acid sites present further in the catalyst bed. This was largely prevented by presaturating the catalyst with ammonia. Therefore, all experiments reported here were performed after presaturation with ammonia.

Figures 6 and 7 compare the results for the amination of ethanol. In Fig. 6 the rate to amines is plotted for each catalyst as a function of temperature. The experiments were performed with 30 mg catalyst and a feed of 40 mbar ethanol and 160 mbar ammonia in He (total flow 10 ml/min). In Fig. 7a, the rates to amines, DEE, and ethylene at 573 K are plotted, and in Fig. 7b, the selectivities to the different amines at 573 K are plotted. These experiments were performed with a feed of 40 mbar ethanol and 160 mbar ammonia, at a total flow of approx. 15 ml/min, but the catalyst weight was varied to achieve a similar conversion over all catalysts of approx. 18%. The overall rate of reaction was the highest over FAU, but the MOR sample showed the highest rate to amines in the temperature region 553–633 K and the highest selectivity at 573 K. The selectivity to ethylene was highest over FAU, while the selectivity to DEE was highest over BEA and SiO_2/Al_2O_3. From the selectivities toward the different amines, it can be seen that FAU had the highest selectivity to TEA and the zeolites with a one-dimensional 12-ring system (MOR and MAZ) the lowest, with BEA assuming an intermediate position. SiO_2/Al_2O_3 exhibited a relatively low TEA selectivity. The MOR samples clearly showed the highest MEA yield of all catalysts tested.

Table 2 compiles the results for ethanol amination over different mordenite catalysts. All experiments were performed over 25–30 mg of catalyst. Experiments 1–5 were performed with $p_{NH3} = 25$ mbar, $p_{EtOH} = 50$ mbar at a total GHSV of 13,000 h^{-1}. Experiments 6–7 were performed at $p_{NH3} = 40$ mbar, $p_{EtOH} = 160$ mbar at a total GHSV of 8000 h^{-1}, and experiment 8 was performed with the same partial pressures of the reactants but at a GHSV of 2500 h^{-1}. Experiments 1 and 2 show that higher reaction

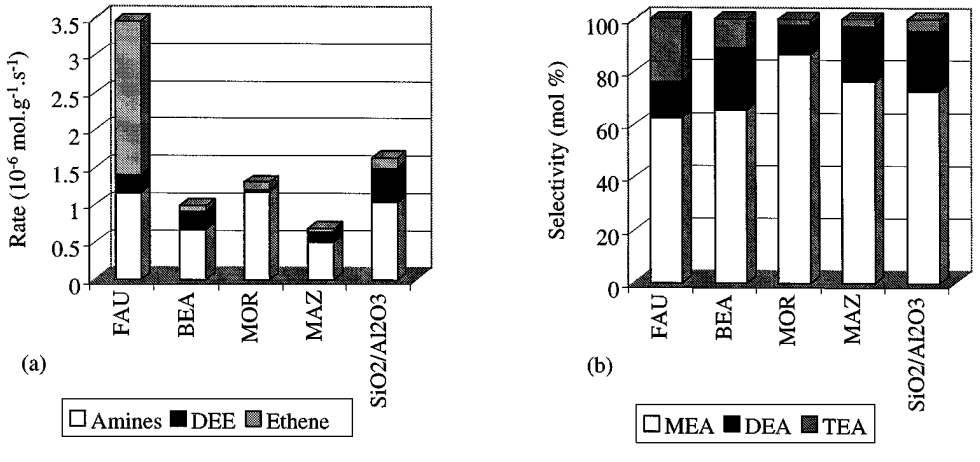

FIG. 7. (a) Rate of product formation and (b) amine selectivity over various catalysts at 15–21% conversion and 573 K.

TABLE 2

Influence of Various Reaction Parameters on Conversion and Selectivity in Ethanol Amination

Exp	Catalyst	T (K)	Reactant ratio[a]	Conv. (%)	Amine select. (%)	Amine distribution (%/%/%)	Ether select. (%)
1	HMOR20	573	1E/2A	5	65	89/10/1	10
2	HMOR20	623	1E/2A	25	40	83/16/1	5
3	HMOR15	573	1E/2A	8	74	84/13/3	8
4	HMOR10	573	1E/2A	9	61	87/12/1	5
5	HMOR10-E	573	1E/2A	15	58	81/16/3	10
6	HMOR15	573	1E/4A	11	84	82/15/3	3
7	HMOR15-M	573	1E/4A	9	93	85/15/0	0
8	HMOR15-M	573	1E/4A	32	92	78/21/1	0

[a] E, ethanol; A, ammonia.

temperatures (expectedly) increased catalyst activity, but decreased the selectivity to amines, mainly due to higher ethene make. Experiments 1 and 3–5 show that for the mordenite-based catalysts, the activities of the catalysts increased in the order HMOR20 < HMOR15 < HMOR10 < HMOR10-E, i.e., parallel to the concentration of available acid sites. HMOR10, which had an anomalously low BET surface area and micropore volume, was less active than the EDTA-treated sample (HMOR10-E). From experiments 3 and 6 it can be seen that increasing the ammonia/ethanol (N/R) ratio from 2 to 4 increased ethanol conversion and amine selectivity. The modified, i.e., silylated, catalyst showed slightly lower activity, but amine selectivity increased from 84 to 93%. DEE formation was negligible when using HMOR15-M and TEA formation was also severely reduced (compare experiments 6 and 7). Higher conversions, achieved by lowering the GHSV, influenced the amine distribution, but did not influence the overall amine selectivity of the catalysts (compare experiments 7 and 8). To explore the influence of the ammonia/ethanol ratio, two experiments were performed in which the ammonia partial pressure was varied relative to a constant ethanol pressure of 50 mbar at 573 K, and one in which it was varied relative to an ethanol pressure of 100 mbar. From these experiments an apparent reaction order of 0.94 in ammonia was obtained.

Optimization of the reaction temperature, the NH_3/ethanol ratio, and the catalyst allowed us to drastically increase the yield to ethylamines at the expense of ethene formation. The results of this optimization are compiled in Fig. 8. Decreasing the reaction temperature enhanced the ethylamine selectivity via a drastic decrease in the rate of ethene formation. The consequential loss in amine yield was compensated by increasing the ammonia partial pressure. As high acid site concentrations and silylation the outer surface of the zeolites were seen to be beneficial to the reaction rate and the amine selectivity (see also Refs. (12, 29)), a material with the maximum acid site concentration (for the MOR materials this was the EDTA treated HMOR10) was used for these modifications. With this strategy HMOR10-EM was prepared showing a 99% selectivity at 60% conversion (250 mg HMOR10-EM, 11 ml/min 100/800 mbar EtOH/NH_3, 558 K).

In general, the mordenite catalysts appeared white after reaction and within the time scale of the experiments (typically 3–4 h), an appreciable deactivation was not observed. In order to test the long-term stability of these catalysts, an amination experiment over HMOR10-EM catalyst (100/800 mbar EtOH/NH_3, 558 K, 0.3 kg amines $kg^{-1}_{catalyst}$ h^{-1} produced at 60% ethanol conversion) was performed for 75 h. The conversion and selectivity as a function of time on stream are depicted in Fig. 9. It can be seen that under these conditions the high selectivity was sustained at stable conversion. The amount of amines produced in this period was approx. 25 kg amines/kg catalyst and the catalyst was still white after use. After 4 h time on stream (1.2 kg amines/kg catalyst produced), the FAU and BEA sample typically showed a slightly grey color.

Because water is one of the reaction products, its influence on the catalyst performance was tested. This was done

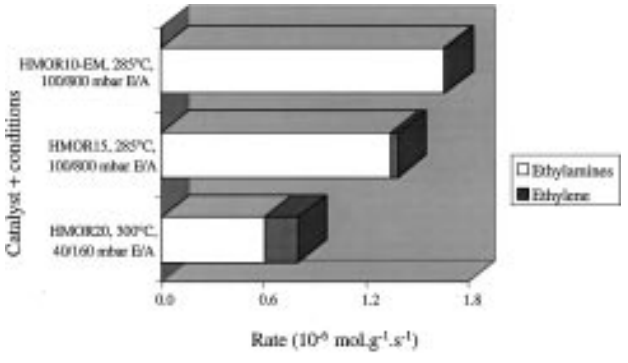

FIG. 8. Optimization of MEA yield by changing catalyst, partial pressures, and temperature.

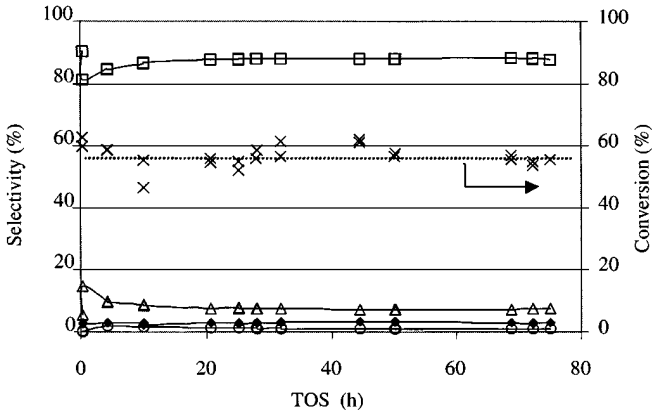

FIG. 9. Stability of HMOR10-EM (558 K, 100/800 mbar EtOH/NH_3). (□) MEA, (△) DEA, (○) TEA, (◆) ethene, and (×) conversion.

by adding 33 mbar of water to the feed of a catalyst at stable operation. As can be seen from Fig. 10, in which the vertical line denotes the time at which water vapor was added to the reaction mixture, the influence of water was negligible.

DISCUSSION

On the Mechanism of Ethanol Amination

As described above, coadsorption of ethanol and ammonia leads to the same coadsorption complex between the ammonium ion and ethanol regardless of the sequence of introduction of the sorbate. The loss of the 3378 cm^{-1} band, assigned to a free N–H stretching vibration (27); the appearance of a band at 3600 cm^{-1}, similar to alcohol adsorption on alkali ions; and the fact that no ammonia is displaced upon introduction of ethanol strongly indicate a coadsorption complex in which ethanol coordinates to NH_4^+ as depicted in Fig. 11. Additionally, TPD after coadsorption (see

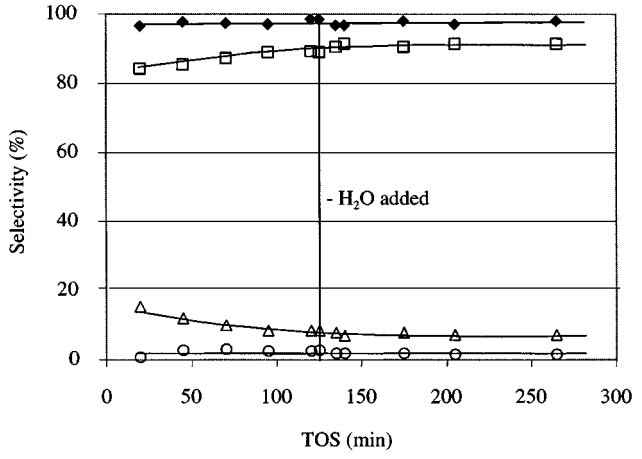

FIG. 10. Influence of water addition (at $t = 120$ min, 558 K, 100/800 mbar EtOH/NH_3). (□) MEA, (△) DEA, (○) TEA, and (◆) total amine selectivity.

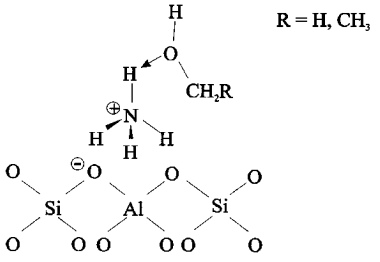

FIG. 11. Coadsorption complex of ethanol and ammonia on acidic catalyst.

Fig. 3) shows that the release of ethanol does not affect the Brønsted acid sites, but restitutes the free N–H stretching band. The bands of the acidic hydroxyl groups of the zeolite are restored only after desorption of ammonia. Note that the proposed coadsorption complex is analogous to the coadsorption complex observed with methanol and ammonia (30, 31). The interaction between the molecules in that complex is rather weak. Consequently, it is not detectable with IR spectroscopy under reaction conditions.

As ammonium ions and weakly adsorbed ethanol suffice to produce alkylammonium ions, we have proposed that under reactive conditions the alkylation of the ammonium ion involves protonation of the alcohol by the ammonium ion, followed by an immediate release of water and the simultaneous formation of a C–N bond (for details see Ref. (29)). The ethylammonium ions resulting from the alkylation of the ammonium ions are very stable, in line with the high base strength of the substituted amines compared to ammonia (32, 33). During the period that the catalyst was exposed to helium or ethanol/helium, amines were not observed in the gas phase. Additional ammonia was needed to remove amines from the surface. This second step, the ammonia-mediated release of amines into the gas phase, is slower than the amine formation; i.e., the initial alkylation of the ammonium ion is fast and the desorption of the formed alkylamine is rate determining. Also the fact that the amination of ethanol is found to be practically first order in ammonia strongly supports a mechanism in which the ammonia-mediated release of amines is rate determining.

The results of the transient experiments for ethanol amination described above are in excellent agreement with those for methanol amination (27). In the latter case, the rate of release of the amines from the surface was also much lower than their initial rate of formation, and reaction orders of approx. 1 (ammonia) and 0 (methanol) have been found (9).

For the ammonia-mediated release of the amines, two types of mechanisms have been proposed: (i) an *alkyl scavenging*-type reaction, in which a gas phase ammonia molecule removes an alkyl group from a sorbed alkylammonium ion, yielding a alkylamine in the gas phase and a sorbed ammonium ion depleted of one alkyl group, and (ii) *adsorption-assisted desorption (a.a.d.)*, in which an

Scavenging: $[R_xNH_y]^+_{ads} + NH_3(g) \rightarrow [R_{x-1}NH_{y+1}]^+_{ads} + RNH_2(g)$

A.a.d.: $[R_xNH_y]^+_{ads} + NH_3(g) \rightarrow [NH_4]^+_{ads} + R_xNH_{y-1}(g)$ where $y = 4 - x$

SCHEME 1. Mechanisms for ammonia-mediated release of amines from acidic catalyst.

incoming ammonia or alkylamine deprotonates the chemisorbed alkylamine which desorbs. Both possible pathways are represented in Scheme 1 and are discussed in detail in Refs. (13, 27).

Differences between the Zeolites

Of the different zeolites investigated, mordenite gave the highest yield to amines, and the rates to ethene and diethyl ether were low compared to the other zeolites tested. This is attributed to the high acidic strength of the mordenite at high acid site concentrations, compared to the other zeolites, which helps to keep the acid sites covered with ammonium ions. This prevents direct elimination of water from ethanol yielding ethene. The much lower rate of DEE formation over MOR is explained by the small pores of MOR and low external acid site concentration disallowing the spatially demanding reaction of two ethanol molecules over a weak acid site. Both subjects will be discussed in detail below.

FAU showed the highest ethanol conversion, but also the by far highest yield to ethene. As it contains the highest concentration of tetrahedrally coordinated aluminum (Brønsted acid sites) and in consequence the highest concentration of Al in next nearest neighborhood to another tetrahedrally coordinated Al, its acid sites are among the weakest of the materials studied (34, 35). This lower acid strength is reflected in the fact that complete removal of ammonia is achieved at temperatures lower than 673 K (compared to 823 K for mordenite). As a consequence ammonia is less stabilized and some free acid sites may be available that catalyze direct ethanol dehydration.

The other zeolites tested had a higher Si/Al ratio and, inferred from the temperature needed for complete ammonia removal (723–823 K), a higher acid strength. The rate of formation of ethene was rather similar for these zeolites. MOR, however, has the highest acid site concentration and, therefore, the highest rate to amines.

All the investigated zeolites have pores with a minimum opening of 12-membered rings. FAU has a three-dimensional channel system connecting the supercages; BEA also has a three dimensional channel system, but no supercages. MOR and MAZ have a one-dimensional 12-ring system and a one-dimensional 8-ring system too small for molecules larger than MEA. For a schematic representation of the molecular sieve channels see Fig. 12. The amine product distribution seems to be related to the dimensionality of the 12-ring system. Selectivity to TEA decreased from 23% over FAU to 10% over BEA and 1–2% over MAZ and MOR. It is speculated that due to the pore structure in FAU with a three-dimensional channel system with rings with an aperture of 0.74 nm and its even larger supercages, diffusion of TEA out of the zeolite particle is relatively facile; i.e., the routes to the outside of the crystallite should be short and numerous and have few obstructions. In BEA, due to the channel structure outlined above, it is more difficult for TEA to exit, but transport will be most difficult in MOR and MAZ since these zeolites have only a one-dimensional large-pore system.

Interesting to note is the significantly lower rate of DEE formation over MOR, compared to the other catalysts. Mordenite has the smallest 12-ring of the samples investigated. It has been shown previously (13) that the formation of ethers proceeds in those circumstances via a concerted reaction between two ethanol molecules over ammonium and alkylammonium ions and depends, thus, on the available pore volume during reaction. Under reaction conditions, the sorbed amines decrease this available volume drastically. The effect of this will be most pronounced in mordenite, since it has the smallest pore diameter. A large external surface area (pronounced meso- and macroporosity) will consequently be unfavorable for low DEE selectivity. In that context we would like to point to the similar performance of amorphous silica/alumina and BEA which both have a similarly large specific external surface area.

Options to Enhance Selectivity

Reaction conditions. In Table 2 it can be seen that upon increasing the temperature from 573 to 623 K the

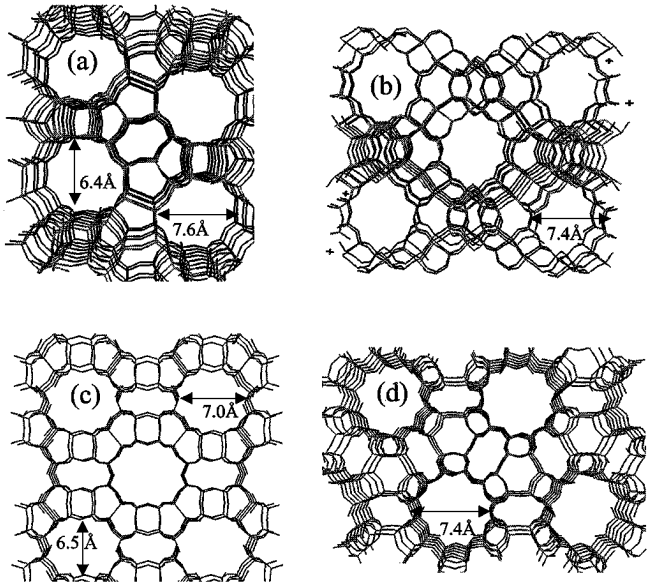

FIG. 12. Zeolite structures, emphasizing the diameter of the 12-ring; (a) BEA, (b) FAU, (c) MOR, and (d) MAZ.

selectivity did not change dramatically. Selectivity to MEA decreased from 89 to 83%, in favor of DEA, which went from 10 to 16%, while TEA selectivity stayed low. Conversion increased from 5 to 25%. As DEA is a secondary product from MEA an increase in DEA selectivity at the expense of MEA can be expected at increasing conversion. The thermodynamic equilibrium composition (as shown in Fig. 1) is slowly shifted from DEA to MEA at increasing temperatures, but this is not expected to have a significant influence since (i) changes over the depicted temperature range (200 K) are not very large, (ii) conversions in the experiments shown are not high enough to approach equilibrium, and (iii) shape selectivity is imposed.

The reaction temperature has a more profound influence on the selectivity to amines than on the amine distribution. Table 2 also shows clearly that the experiment performed at 623 K had a significantly lower selectivity to amines than the experiment at 573 K. With all acid sites covered by alkylammonium ions under these conditions this suggests that the decomposition of the ethylammonium ions, as found in the TPD experiments, poses a problem for ethanol amination at temperatures above 573 K. The rates of this reaction seem to approach the rates for the ammonia-mediated desorption pathways and consequently decrease the selectivity to amines. It should be noted that in the absence of ammonia this decomposition is quantitative and has been been used to determine acid site concentrations (32). As a consequence all reactions discussed were therefore carried out at or below 573 K.

In order to maximize the selectivity to amines, not only formation of ethylene via Hoffmann elimination has to be suppressed, but also the elimination of water from ethanol, leading to ether or ethylene. Experiments with ethanol as single feed indicate that the rate of ethene formation is more than two orders of magnitude higher than the rate of amine formation ($>10^{-4}$ mol g^{-1} s^{-1} vs 10^{-6} mol g^{-1} s^{-1}). Thus, only a small fraction of free acid sites suffice to catalyze the conversion of a significant fraction of ethanol to ethene. This can be minimized by (i) high ratios of ammonia to ethanol (compare experiments 3 and 6 in Table 2), (ii) a strongly acidic zeolite (high stability of the ammonium ions; compare results for mordenite and zeolite Y), and (iii) low reaction temperatures (compare experiments 1 and 2 in Table 2). In the latter case, three factors help to suppress ethene formation; the thermodynamic equilibrium favors ethanol at lower temperatures (see Fig. 1b), the relative adsorption constant of ammonia is higher, and formation of ethylene via Hoffmann elimination is minimized.

Another route to ethene could be the decomposition of DEE. If formation of ethene from DEE were much faster than Hoffman elimination, i.e., a major pathway, then DEE and ethene selectivities should be more or less parallel. However, when comparing DEE and ethene formation for example over MOR and BEA or over MOR in experiments 3 and 4 of Table 2, we see that they are not parallel. This would indicate that formation of ethene from DEE is not a major pathway during amination of ethanol.

Silylation of the outer surface of the mordenite crystallites. As outlined before (6, 11–13), silylation of the outer surface of a molecular sieve generates a thin silica layer blanketing the acid sites of the outer surface and decreasing the diameter of the pore mouth opening. With mordenite this has been shown to be very effective for enhancing the selectivity to methylamines in general and to monomethylamine in particular. Thus, one might expect that the treatment has a similar positive effect upon ethylamine synthesis.

Table 2 (comparing experiments 6 and 7) shows that silylation drastically reduces the ether formation. The selectivity to amines in general and the monosubstituted product in particular were significantly enhanced. Despite a slightly lower rate of total alcohol conversion, this results in an increase of the rate of mono-alkylamine formation, as illustrated in Fig. 13. There, it can be seen that the formation of MEA (primary product) is approximately first order in the acid site concentration for the nonsilylated mordenite series. Silylation of the outer surface, however, slightly enhances the rate of formation of MEA. The decreased pore mouth diameter hinders the higher substituted amines to leave the pores, thereby generating a higher degree of alkylation of alkylammonium ions. In methanol amination these were found to be more reactive than lower substituted ammonium ions (12, 13). The smaller pore mouth could also enhance the concentration of reactants in the zeolite and thereby enhance the reaction rate.

Also the use of ethanol is more efficient since diethyl ether is not formed over the silylated catalyst. As discussed above, formation of ethers under amination conditions has been found to proceed mainly over the sorbed ammonium ions (13). As silylation causes a decrease in the size of the pore mouth and the elimination of external acid sites, it exerts two positive effects. The narrowing of the pore

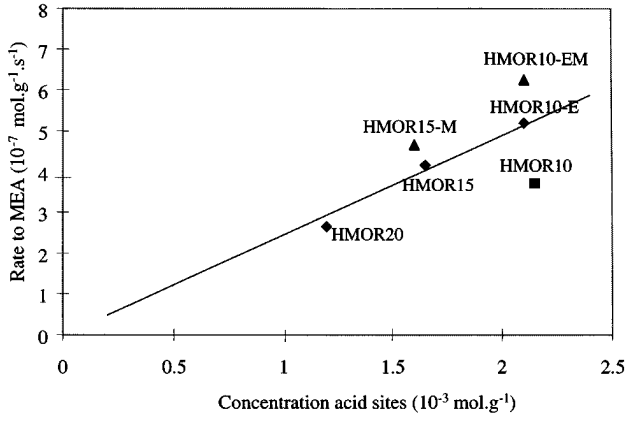

FIG. 13. Influence of catalyst treatment on rate of MEA formation.

opening effectively increases the substitution of the alkylammonium ions in the pores and decreases the internal available pore volume for the concerted bimolecular DEE formation. On the other hand it also blocks strong acid sites on the outer surface and so suppresses formation of alkylammonium ions that may also catalyze DEE formation.

Deactivation

Two factors are important in the prevention of coking. (i) The suppression of olefin formation and (ii) the prevention of olefin oligomerization to form stable species inside the zeolite. The stability of the HMOR10-EM catalyst is very good. No appreciable decrease in activity and selectivity after 75 h and no discoloration of the catalyst after use were observed. We observed some formation of olefinic species by IR spectroscopy, but no pronounced coking or deactivation. The two reasons we propose for the high stability of especially the modified mordenite are (i) the overall strength of the acid sites and (ii) the pore structure.

Coke precursor formation is greatly impeded by stabilization of the ammonium ions due to the strength of the acid sites. This effect is enhanced by the relatively large concentration of higher ethylammonium ions present inside the pores of the silylated material and the one-dimensional nature of the mordenite pores. These higher ethylammonium ions are even more strongly adsorbed than ammonium ions, providing a very effective shielding of the acid sites from (i) ethanol and (ii) the small amounts of ethylene produced, thereby inhibiting the formation of coke precursors.

Mordenite has often been described as being very susceptible to coke formation (36), mainly due to the one-dimensional nature of the pore system in which a relatively small number of obstructions can render a large portion of the pore system inaccessible. Our results, however, indicate that modified mordenite is one of the most stable catalysts for amination reactions. The formation of larger, stable coke species can be inhibited by the geometrical constraints due to pore structure. This space is even more confined in the case of modified mordenite due to the increased substitution of ammonium ions at the acid sites.

FAU has much weaker acid sites and selectivity to olefins is high. This fulfills one of the conditions for coke formation: the presence of precursors in the form of olefinic species. The oligomerization process can also be facilitated by the higher availability of free acid sites. The specific shape of the FAU structure with its large supercages facilitates the formation of larger, more complex molecules which can easily become trapped within the zeolite.

CONCLUSIONS

Amination of ethanol over acidic catalysts has been shown to proceed in two steps. The first step consists of the alkylation of ammonium ions by ethanol and the second, rate determining, step is the ammonia-mediated release of the formed amines (sorbed as alkylammonium ions) into the gas phase. The precursor to this reaction is proposed to be a coadsorption complex in which ethanol coordinates with its oxygen atom to the ammonium ion on the acid site. After the formation of this complex, protonation of the ethanol from the ammonium ion occurs, followed by release of water and the formation of a C–N bond. These steps are similar to those reported for methanol amination (12, 29, 27).

Because the ethyl group is a better leaving group than the methyl group, ethene formation from ethanol, diethyl ether, and the ethylammonium ammonium ion is facile. Formation of ethene is, thus, the main problem in solid acid-catalyzed ethanol amination. It can be suppressed by applying high ammonia partial pressures and low reaction temperatures, and by choice of a proper catalyst, i.e., a molecular sieve that has narrow pores and stabilizes (alkyl)ammonium ions well.

The influence of the ammonia concentration is twofold: (i) ethanol amination has a positive order in $p(NH_3)$ of 0.94 for the formation of amines and (ii) high ammonia pressures will minimize direct exposure of ethanol to acid sites leading to ethene formation.

Low reaction temperatures are necessary, as TPD of alkylamines shows that above 573 K ethylamines start to decompose at an appreciable rate to ethene and ammonia. For a given ammonia partial pressure lower temperatures help to maintain the acid sites covered with ammonium ions, preventing direct access of ethanol or DEE.

Comparison of the acid catalysts studied shows conclusively that the catalyst properties influence the overall amine selectivity and the selectivity within the amines. With respect to the first point, chemical composition and pore geometry are found to be the crucial parameters. Zeolites with a low Si/Al ratio, which are weaker solid acids and do not stabilize ethylammonium ions well, show a higher tendency to form ethene. This is attributed to the presence of free acid sites which catalyze the formation of ethene due to ethanol or DEE dehydration. It should be noted at this point, however, that the rate of amination sympathetically varies with the concentration of acid sites and that an optimum Si/Al ratio exists as a consequence. This is exemplified clearly by the low amine yield found with FAU (Si/Al = 2.7) having the lowest yields and rates in ethylamines and the high yields found with HMOR10-EM (Si/Al = 5). In that context, the temperature needed for complete ammonia removal during activation of the sample, as observed with FTIR, seems to be a good indication of whether the chosen catalyst will show a good amine selectivity. If complete ammonia removal takes place below 723 K, the catalyst will likely show high ethene selectvities.

The pore structure of the zeolite has a definite influence on amine selectivity and amine distribution. If the acid sites

are in a relatively confined space, as in MOR, which had the smallest channels of the zeolites investigated, the available space for ether formation over weakly acidic centers will be lower and consequently the rate to DEE will decrease. The rate to TEA is greatly influenced by the diffusional constraints imposed on the products. FAU, with its open, three-dimensional pore system, had the highest TEA selectivity (23%), whereas MOR and MAZ, with their one-dimensional pore system, produced much less TMA (1–2%).

The most promising way of enhancing MEA yield is silylation of the outer surface of the mordenite. Although the overall conversion drops slightly, selectivity to by-products (especially diethyl ether) decreased and the MEA yield increased. This is attributed to a decrease in available pore volume for the bimolecular alcohol dehydration reaction caused by increasing substitution of the alkylammonium ions and the elimination of accessible Brønsted acid sites or alkylammonium ions on the outer surface of the molecular sieve crystals.

ACKNOWLEDGMENT

This work was performed under the auspices of NIOK, The Netherlands Institute for Catalysis Research, Lab. Report UT-98-1-08.

REFERENCES

1. Heilen, G., Mercker, H. J., Frank, D., Reck, R. A., and Jäckh, R., *in* "Ullmann's Encyclopedia of Industrial Chemistry" (W. Gerhertz, Ed.), 5th ed., Vol. A2, p. 1. VCH, Weinheim, 1985.
2. Turcotte, M. G., and Johnson, T. A., *in* "Kirk Othmer Encyclopedia of Chemical Technology" (J. J. Kroschwitz, Ed.), 4th ed., Vol. 2, p. 369. Wiley, New York, 1992.
3. Corbin, D. R., Schwarz, S., and Sonnichsen, G. C., *Catal. Today* **37**, 71 (1997).
4. Ashina, Y., Fujita, T., Fukatsu, M., Niwa, K., and Yagi, Y., *Stud. Surf. Sci. Catal.* **84**, 28,779 (1986).
5. Shannon, R. D., Keane, M., Jr., Abrams, L., Staley, R. H., Gier, T. E., Corbin, D. R., and Sonnichsen, G. C., *J. Catal.* **113**, 367 (1988).
6. Segawa, K., and Tachibana, H., *J. Catal.* **131**, 482 (1991).
7. Ilao, M. C., Yamamoto, H., and Segawa, K., *J. Catal.* **161**, 20 (1996).
8. Dingerdissen, U., Nagy, E., and Fetting, F., *Chem. Ing. Technol.* **63**, 625 (1991).
9. Chen, D. T., Zhang, L., Kobe, J. M., Yi, C., and Dumesic, J. A., *J. Mol. Catal.* **93**, 337 (1994).
10. Ashina, Y., and Fukatsu, M., U.S. Patent 4,485,261 (1984).
11. Niwa, M., Kato, S., Hattori, T., and Murakami, Y., *J. Chem. Soc. Faraday Trans 1* **80**, 3135 (1984).
12. Gründling, Ch., Eder-Mirth, G., and Lercher, J. A., *J. Catal.* **160**, 299 (1996).
13. Veefkind, V. A., Gründling, Ch., and Lercher, J. A., *J. Mol. Catal. A* **134**, 111 (1998).
14. Kaeding, W. W., U.S. Patent 4,082,805 (1978).
15. Deeba, M., Ford, M. E., and Johnson, T. A., *in* "Catalysis of Organic Reactions" (W. Blackburn, Ed.). Dekker, New York, 1990.
16. Shen, J.-P., Ma, J., Jiang, D.-Z., and Min, E.-Z., *Chinese Chem. Lett.* **5**, 305 (1994).
17. Sawa, M., Niwa, M., and Murikami, Y., *Zeolites* **10**, 532 (1990).
18. Pirngruber, G. D., Eder-Mirth, G., and Lercher, J. A., *J. Phys. Chem.* **101**, 561 (1997).
19. Nivarthy, G. S., He, Y., Seshan, K., and Lercher, J. A., *J. Catal.* **176**, 192 (1998).
20. Stockenhuber, M., and Lercher, J. A., *Microporous Mater.* **3**, 457 (1995).
21. Mirth, G., Eder, F., and Lercher, J. A., *Appl. Spectrosc.* **48**, 194 (1994).
22. Blaszkowski, S. R., and van Santen, R. A., *J. Phys. Chem.* **99**, 11728 (1995).
23. Zecchina, A., and Otero Arean, C., *Catal. Rev.* **35**, 261 (1993).
24. Thursfield, A., and Anderson, M. W., *J. Phys. Chem.* **100**, 6698 (1996).
25. Mirth, G., Lercher, J. A., Anderson, M. W., and Klinowski, J., *J. Chem. Soc. Faraday Trans.* **86**, 3039 (1990).
26. Little, L. H., "Infrared Spectra of Adsorbed Species," p. 180. Academic Press, London, 1966.
27. Kogelbauer, A., Lercher, J. A., Steinberg, K. H., Roessner, F., Soellner, A., and Dimitriev, R. V., *J. Chem. Soc. Faraday Trans.* **88**, 2283 (1992).
28. Gründling, Ch., Eder-Mirth, G., and Lercher, J. A., *Res. Chem. Intermediates* **23**, 25 (1997).
29. Segawa, K., and Tachibana, H., *in* "Proceedings, 10th ICC," p. 1273. Elsevier, Amsterdam, 1993.
30. Kogelbauer, A., Gründling, Ch., and Lercher, J. A., *J. Phys. Chem.* **100**, 1852 (1996).
31. Gründling, Ch., Veefkind, V. A., Eder-Mirth, G., and Lercher, J. A., *Stud. Surf. Sci. Catal.* **105**, 591 (1997).
32. Parillo, D. J., Adamo, A. T., Kokatailo, G. T., and Gorte, R. J., *Appl. Catal.* **67**, 107 (1990).
33. Parillo, D. J., Gorte, R. J., and Farneth, W. E., *J. Am. Chem. Soc.* **115**, 12441 (1993).
34. Makarova, M. A., Zholobenko, V. L., Al-Ghefaili, K. M., Thompson, N. E., Dewing, J., and Dwyer, J., *J. Chem. Soc. Faraday Trans.* **90**, 1047 (1994).
35. Parillo, D. J., and Gorte, R. J., *J. Phys. Chem.* **97**, 8786 (1993).
36. Magnoux, P., Cartraud, P., Mignard, S., and Guisnet, M., *J. Catal.* **106**, 242 (1987).